Hindawi
Journal of Advanced Transportation
Volume 2017, Article ID 3506053, 19 pages
https://doi.org/10.1155/2017/3506053

Research Article

Bifurcation of Lane Change and Control on Highway for Tractor-Semitrailer under Rainy Weather

Tao Peng,[1] Zhiwei Guan,[1] Ronghui Zhang,[2] Jinsong Dong,[3] Kening Li,[4] and Hongguo Xu[5]

[1]*College of Automobile and Transportation, Tianjin University of Technology and Education, Tianjin 300222, China*
[2]*Guangdong Key Laboratory of Intelligent Transportation System and Research Center of Intelligent Transportation System, School of Engineering, Sun Yat-sen University, Guangzhou 510275, China*
[3]*Key Laboratory of Operation Safety Technology on Transport Vehicles, Research Institute of Highway Ministry of Transport, Beijing 100088, China*
[4]*State Key Laboratory of Mechanical System and Vibration, School of Mechanical Engineering, Shanghai Jiaotong University, Shanghai 200240, China*
[5]*College of Transportation, Jilin University, Changchun 130025, China*

Correspondence should be addressed to Ronghui Zhang; zrh1981819@126.com

Received 7 July 2017; Accepted 5 September 2017; Published 19 October 2017

Academic Editor: Cheng S. Chin

A new method is proposed for analyzing the nonlinear dynamics and stability in lane changes on highways for tractor-semitrailer under rainy weather. Unlike most of the literature associated with a simulated linear dynamic model for tractor-semitrailers steady steering on dry road, a verified 5DOF mechanical model with nonlinear tire based on vehicle test was used in the lane change simulation on low adhesion coefficient road. According to Jacobian matrix eigenvalues of the vehicle model, bifurcations of steady steering and sinusoidal steering on highways under rainy weather were investigated using a numerical method. Furthermore, based on feedback linearization theory, taking the tractor yaw rate and joint angle as control objects, a feedback linearization controller combined with AFS and DYC was established. The numerical simulation results reveal that Hopf bifurcations are identified in steady and sinusoidal steering conditions, which translate into an oscillatory behavior leading to instability. And simulations of urgent step and single-lane change in high velocity show that the designed controller has good effects on eliminating bifurcations and improving lateral stability of tractor-semitrailer, during lane changing on highway under rainy weather. It is a valuable reference for safety design of tractor-semitrailers to improve the traffic safety with driver-vehicle-road closed-loop system.

1. Introduction

Tractor-semitrailer, as an articulated vehicle system, has complex nonlinear dynamic characteristics. Vehicle dynamics bifurcation mechanisms and driving stability have basically been confirmed based on nonlinear theory and tire mechanics. Early works on this subject have established three degrees of freedom (DOF) dynamic model with simplified nonlinear tire formula, which are essential for a clear understanding of the system's nonlinear stability [1, 2]. Due to the special articulated structure, jackknife and coordination stability have drawn wide attention. Dunn et al. rigorously developed a 15-state model using Lagrange's method and studied in detail the effects on jackknife stability when using brakes under different road adhesion coefficients [3–5]. To protect the vehicle from spinning and realize improved cornering performance, van de Molengraft-Luijten et al. employed the Routh-Hurwitz stability criterion and bifurcation theory method to get a system equilibrium approximation near the zero value for the forward speed and front wheel steering angle, which revealed the vehicle's instability under high speeds and substantial steering [6, 7]. Similarly, Ding et al. explained some instability phenomena of the vehicle system such as jackknifing, sideslip, and spinning by correlating them with the behavior in the neighborhood of unstable fixed points based on analysis of eigenvectors, phase trajectories, and status of lateral tire force saturation [8]. Sadri and Wu investigated Lyapunov concept exponents and applications to

analyze the stability for the nonlinear vehicle in plane motion with a third-order polynomial tire model [9]. In addition, the existing literatures focus on bifurcation application analysis for the stability assessment of a complex railway vehicle model [10, 11].

Moreover, vehicle/driver and vehicle/driver/road cooperation systems and influence parameters were introduced for tractor-semitrailer nonlinearity investigations [12–15]. To study vehicle Hopf bifurcation and chaos characteristics and variation in pilot model parameters and to discuss the qualitative motion behavior near the critical speed, Rossa et al. proposed a simple 3DOF closed-loop vehicle/driver model [16, 17]. Li et al. presented a nonlinear vehicle-road coupled model and analyzed the dynamic behaviors of a nonlinear system using a numerical integration method [18]. With a closed-loop system of articulated heavy vehicles with driver steering control, Liu et al. employed an integration method to derive an analytical periodic solution of the system in the neighborhood of the critical speed and analyzed supercritical and subcritical Hopf bifurcations [19]. Koglbauer et al. paid close attention to drivers' workload and effort in different road conditions [20]. Bie et al. proposes a weather factor model built by introducing weather factors to free flow speed, capacity, and critical density and plugged it into traffic control [21]. Tang et al. investigated the road condition and driver characteristics on the lane change driving trajectory and traffic safety, such as lane number, driver's time delay, and perception ability effect [22–27]. Related researches are helpful to master the interactions of vehicle, driver, and work environment.

Furthermore, with the rapid development of control theory, a variety of methods are available in the tractor-semitrailer stability control system and product, such as ABS (Antilock Brake System) and ESC (Electronic Stability Control). By an optimal control approach for driver model, Liu studied the stability of a time delayed dynamical tractor-semitrailer, using a numerical method by computing the eigenvalues near the imaginary axis [13]. Lin et al. proposed optimal linear quadratic control algorithm to improve the yaw stability of a tractor semitrailer using active semitrailer steering [28]. Palkovics and El-Gindy applied RLQR/H_∞ approach to ensure the vehicle's performance in the presence of parametric uncertainties and discussed the influence of different control strategies on the vehicle's directional and roll stability during severe path-follow lane change manoeuvre [29]. Chang et al. designed a H_∞ loop shaping robust controller robust of tractor-semitrailer, which provides a novel mean or method for explore tracking control problem of the tractor-semitrailer [30]. Liang et al. proposed a specified fuzzy sliding mode controller to guarantee the robust control in the presence of system uncertainties [31]. By active wheel braking, Takenaga et al. proposed a novel fuzzy logic based yaw moment controllers to track the reference yaw rate of the tractor and the hitch angle and demonstrated the robust and effects in stabilizing the severe instabilities such as jackknife and trailer oscillation in the chosen simulation scenarios [32–34]. Zong et al. applied a multiobjective stability control algorithm to improve the vehicle stability of a tractor semitrailer by using differential braking [35]. Recently, more and more people pay attention to intelligent vehicle based on Cooperative Vehicle Infrastructure System [36–43]. Besides, vehicle control and system model was combined with transportation simulation [44–52].

Many of the conclusions of the classical literature play a positive role in vehicle handing stability. However, there are still some limitations, especially in particular research backgrounds. First, it is clear that the vehicle instability in critical conditions is mainly due to the nonlinearity of tires, but most of traditional vehicle dynamics models are deduced by simplified tire formulas. The convenient calculations still deviate greatly from reality. Second, previous research on vehicles' characteristics has concentrated on steady steering [53–56]. However, lane changes and overtaking by heavy trucks on highways, as a frequent driving behavior, could gain more attention in the near future. Furthermore, most of the traditional efforts have focused on vehicle stability on common road [57, 58]. In fact, rainy weather and lower adhesion coefficient should be taken into consideration, especially for heavy trucks.

Tractor-semitrailer, as a very important and highly effective means of freight transportation, is more dangerous than general passenger cars because of their articulated structure, large size, and difficult handling. Accidents involving tractor-semitrailers tend to cause serious casualties and losses. Therefore, active safety and traffic transportation researchers have paid more attention to tractor-semitrailers' driving stability in recent years. In particular, lane changing is a common driving behavior on highways, but high speeds and large-scale continuous steering can easily cause stability losses, such as sideslips and nonlinear oscillatory, for tractor-semitrailers. Last but not least, considering the large-scale rainy season in the south of our country, vehicles driving on lower adhesion efficient road and harsh environment are common, which cause increased instability and traffic accidents [59–63]. Therefore, nonlinear analysis and control of tractor-semitrailers' lane changing on highways under rainy weather have important practical significance in the vehicle dynamics research field and provide a valuable reference for active safety design.

This work deals with the nonlinear dynamics and control of tractor-semitrailers changing lanes on highways under rainy weather, which is a highly relevant real-life situation. In order to master the essence of stability and instability mechanism of tractor-semitrailer changing lanes at high speed, Rough-Hurwitz stability criterion is developed to analyze vehicle transient stability, and the vehicle bifurcation characteristics under steady and transient steering are studied based on nonlinear theory. In view of the vehicle's instability mechanism, feedback linearization control model is deduced and controller combined with AFS (Active Front Steering) and DYC (Direct Yaw Control) was established and presented. It is significant to provide a valuable reference for safety design of tractor-semitrailers, to improve the traffic safety of driver-vehicle-road closed-loop system.

This text is structured as follows: after a brief description of the vehicle model and validation in Section 2, Section 3 analyzes bifurcations with steady steering and sinusoidal steering to simulate the main process of lane changing.

Section 4 deals with an investigation of feedback linearization control for lane changing. Section 5 proposes a conclusion and further work. Conflicts of interest and acknowledgements are dealt with at the end of the article.

2. Vehicle System Model

By defining ground coordinate system XOY, Figure 1 illustrates the plane motion force diagrams of tractor and semitrailer vehicle coordinate systems $x_to_ty_t$ and $x_so_sy_s$. The x_t and x_s axes, respectively, point forward and lie both in the ground plane and in the plane normal to the ground of tractor and semitrailer. The y_t and y_s axes point to the left. Positions of o_t and o_s are, respectively, centroid of the vehicles. As motion variables we define the longitudinal velocities v_{xt} and v_{xs}, lateral velocities v_{yt} and v_{ys} of tractor and semitrailer centroids, the slip angles β_t and β_s are respectively introduced by longitudinal and lateral velocities of tractor and semitrailer, the yaw angles φ_t and φ_s are respectively included angles between longitudinal axes and x_s and x_t axes of tractor and semitrailer.

As shown in Figure 1, when front wheels are steering, the vehicle is not only moving along the longitudinal direction, but also introduced the lateral motion around the steering center, and the yaw motion caused by dynamic centrifugal force at centroid. Thus, 5DOF model involves steering system motion, tractor, and semitrailer's longitudinal and lateral motions, and yaw motions could be depicted in Figure 1. During the process, forces acting on the tires provide centripetal force of vehicle motion. In common situation, the centrifugal force is balanced with the centripetal force, and the plane motions of the vehicle will be in a regular way. Otherwise, if the centrifugal force is greater than the centripetal force, the vehicle will sideslip.

2.1. Vehicle Dynamics Model. Considering the research vehicle is moving on highway when steering without active braking and the road is flat, but wet and slippery under rainy weather, vertical, roll, and pitch motion can be ignored in this situation. Thus, the established vehicle model could be simplified as 5DOF model. The corresponding equations of the vehicle model are as follows:

(1) Tractor,

$$\begin{aligned} m_t\left(\dot{v}_{xt} + v_{yt}\dot{\varphi}_t\right) &= F_{xtf} + F_{xtr} - F_{xth},\\ m_t\left(\dot{v}_{yt} + v_{xt}\dot{\varphi}_t\right) &= F_{ytf} + F_{ytr} - F_{yth},\\ I_{zt}\ddot{\varphi}_t &= a_tF_{ytf} - b_tF_{ytr} + cF_{yth}. \end{aligned} \tag{1}$$

(2) Semitrailer,

$$\begin{aligned} m_s\left(\dot{v}_{xs} + v_{ys}\dot{\varphi}_s\right) &= F_{xs} + F_{xsh},\\ m_s\left(\dot{v}_{ys} + v_{xs}\dot{\varphi}_s\right) &= F_{ys} + F_{ysh},\\ I_{zs}\ddot{\varphi}_s &= -b_sF_{ys} + a_sF_{ysh}. \end{aligned} \tag{2}$$

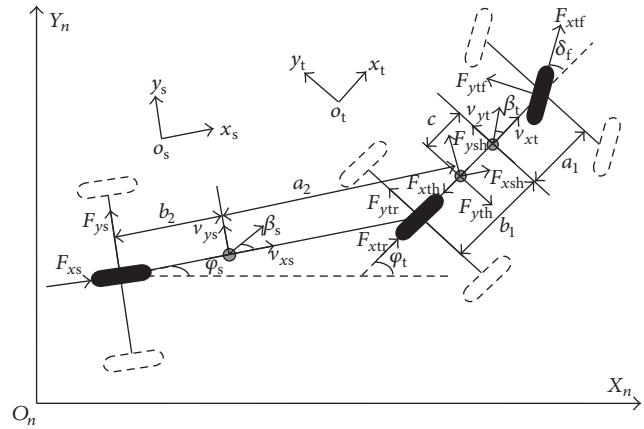

F_{xtf}: longitudinal force of tractor front wheels
F_{ytf}: lateral force of tractor front wheels
F_{xtr}: longitudinal force of tractor rear wheels
F_{ytr}: lateral l force of tractor rear wheels
F_{xs}: longitudinal force of semitrailer wheels
F_{ys}: lateral force of semitrailer wheels
$F_{xt(s)h}$: longitudinal force of tractor (semitrailer) on saddle
$F_{yt(s)h}$: lateral force of tractor (semitrailer) on saddle
δ_f: front wheel steering angle
$\beta_{t(s)}$: slip angle of tractor (semitrailer) centroid
$v_{xt(s)}$: longitudinal velocity of tractor (semitrailer) centroid
$v_{yt(s)}$: lateral velocity of tractor (semitrailer) centroid
$\varphi_{t(s)}$: yaw angle of tractor (semitrailer)
a_t: distance between tractor centroid and front axle
b_t: distance between tractor centroid and rear axle
c: distance between tractor centroid and saddle point
a_s: distance between semitrailer centroid and front axle
b_s: distance between semitrailer centroid and rear axle

Figure 1: Schematic diagram of tractor-semitrailer plane motion.

(3) Steering system [64],

$$I_w\ddot{\delta}_f + C_w\dot{\delta}_f = K_w\left(\frac{\delta_{sw}}{i} - \delta_f\right) - \varepsilon F_{ytf}. \tag{3}$$

Meanwhile, conditions of saddle balance approximately satisfy

$$\begin{aligned} v_{xt} &= v_{xs},\\ v_{ys} &= v_{xt}\theta + v_{yt} - \left(c + a_s\right)\dot{\varphi}_t + a_s\dot{\theta},\\ F_{xth} &= F_{xsh},\\ F_{yth} &= F_{ysh}. \end{aligned} \tag{4}$$

Taking a domestic tractor-semitrailer as an example, relevant vehicle parameters and symbols are listed in Table 1. Here, the mass and structure values of the vehicle refer to test data, inertia, and stiffness and the other performance data are selected based on database of Trucksim.

2.2. Nonlinear Tire Model. In addition to supporting the vehicle steering dynamics, the tires provide the lateral forces necessary to change the speed and direction of the vehicle.

Table 1: Tractor-semitrailer parameters and symbols.

Symbol	Parameter name	Value	Unit
m_t	Tractor mass	5800	kg
m_s	Semitrailer mass	19080	kg
a_t	Distance between tractor centroid and front axle	2.0	m
b_t	Distance between tractor centroid and rear axle	1.4	m
c	Distance between tractor centroid and saddle point	0.8	m
a_s	Distance between semitrailer centroid and saddle point	2.0	m
b_s	Distance between semitrailer centroid and rear axle	1.4	m
I_{zt}	Tractor yaw moment of inertia	9737	kg·m^2
I_{zs}	Semitrailer yaw moment of inertia	138437	kg·m^2
I_w	Moment of inertia of steering wheel around spin	60	kg·m^2
C_w	Damping coefficient of steering wheel around spin	10250	—
K_w	Steering system stiffness	2000	Nm/rad
ε	Tractor front tire pneumatic trail	0.01	m
i	Steering radio	28	—
v_{xt}	Tractor longitudinal velocity	—	m/s
v_{xs}	Semitrailer longitudinal velocity	—	m/s
v_{yt}	Tractor lateral velocity	—	m/s
v_{ys}	Semitrailer lateral velocity	—	m/s
φ_t	Tractor yaw angle	—	rad/s
φ_s	Semitrailer yaw angle	—	rad/s
θ	Articulated angle	—	rad
δ_{sw}	Tractor steering wheel angle	—	rad
δ_f	Tractor front wheel steering angle	—	rad
F_{xtf}	Tractor front wheel longitudinal force	—	N
F_{xtr}	Tractor rear wheel longitudinal force	—	N
F_{ytf}	Tractor front wheel lateral force	—	N
F_{ytr}	Tractor rear wheel lateral force	—	N
F_{xs}	Semitrailer wheel longitudinal force	—	N
F_{ys}	Semitrailer front wheel lateral force	—	N
F_{xth}	Longitudinal force from saddle to tractor	—	N
F_{yth}	Lateral force from saddle to tractor	—	N
F_{xsh}	Longitudinal force from saddle to semitrailer	—	N
F_{ysh}	Lateral force from saddle to semitrailer	—	N

There exist many tire models to describe tire behaviors beyond the linear region. One model commonly used in vehicle dynamics simulations was developed by Pacejka of the Delft University of Technology [64, 65]. The lateral slip angle α generates a lateral force, F_y, at the tire-ground interface, which could be expressed as a magic formula:

$$F_y = D \sin\left(C \operatorname{atan}\left\{B\alpha - E\left[B\alpha - \operatorname{atan}\left(B\alpha\right)\right]\right\}\right), \quad (5)$$

where α is the tire slip angle and B, C, D, and E are, respectively, the stiffness factor, shape factor, peak factor, and curvature factor.

As we know, sideslip instability of a tractor-semitrailer is caused by exceeding the lateral tire force saturation. Lower lateral tire force saturation arises from lower adhesion coefficient under rainy weather, which easily causes severe nonlinear performance of the vehicle. Normally, on wet and slippery road, the absolute value of peak factor D must be lower and the stiffness and shape factors (B and C) are higher than that on general roads. Relevant parameters valued as all wheels of each axis on wet road ($\mu = 0.3$) for the tires are listed in Table 2 [66].

Table 2: Values of B, C, D, and E for a nonlinear tire.

Tire position	Tire number	B	C	D	E
Tractor front wheel	2	3.32	1.2	−12987.6	−1.45
Tractor rear wheel	4	11.35	1.2	−16327.2	−1.45
Semitrailer wheel	8	19.62	1.2	−25792.8	−1.45

Figure 2: Image of vehicle test environment.

These slip angles may be obtained using the following handing relations:

$$\alpha_{tf} = \arctan\left(\frac{v_{yt} + a_t\omega_t}{v_{xt}}\right) - \delta_f,$$
$$\alpha_{tr} = \arctan\left(\frac{v_{yt} - b_t\omega_t}{v_{xt}}\right), \quad (6)$$
$$\alpha_s = \arctan\left(\frac{v_{ys} - b_s\omega_s}{v_{xs}}\right),$$

where α_{tf}, α_{tr}, and α_s are, respectively, the tractor front and rear wheel and the semitrailer wheel's slip angle, v_{yt} and v_{ys} are, respectively, the tractor and semitrailer's lateral velocity, v_{xt} and v_{xs} are, respectively, the tractor and semitrailer's longitudinal velocity, a_t is the distance between tractor centroid and front axle, b_t is distance between tractor centroid and rear axle, b_s is the distance between semitrailer centroid and rear axle, and ω_t and ω_s are, respectively, the tractor and semitrailer's yaw rate.

2.3. Vehicle Dynamics Model Validation. The double-lane change is deemed the general method of overtaking. The whole process can be divided into five steps: straight driving in original lane, approximately sinusoidal steering, straight driving in the other lane, and approximately sinusoidal steering and steer returning in original lane. Thus, the tractor-semitrailer comes under complex and severe dynamics, with changes in lane position, large-scale continuous steering, and high speed.

To validate the vehicle dynamics model, applying a domestic tractor-semitrailer, we conducted a physical double-lane change experiment on an even and wet road, just as a tractor-semitrailer overtaking under rainy weather on highway. Tests were carried out at a professional test site in the Key Laboratory of Operation Safety Technology for Transport Vehicles, at the Research Institute of the Highway Ministry of Transport, Beijing, China. Details of the test environment are shown in Figure 2.

The tested vehicle was driven along the double-change channel on an even and wet road, with its velocity kept to about 60 km/h. The integrated test system mainly involved a VBOX III for tractor, a VBOX II and an inertial sensor for semitrailer, a vehicle-handling force and angle meter for vehicle steering, a data collection device, and a power supply device, whose function was to measure the steering wheel angle input and the output vehicle motion parameters, including velocity, acceleration, and angular velocity.

Setting the simulation inputs the same as test velocities and steering wheel angles, in addition, the time step is 0.05 s in accord with test sampling frequency 20 Hz. Furthermore, the orientations of simulated output variables keep consistent with test.

Under the same conditions, tractor and semitrailer lateral accelerations, yaw rates, and joint angle were obtained using vehicle testing and Matlab simulation and compared, as shown in Figure 3.

Clearly, the vehicle's lateral and yaw dynamics in Figure 3 exhibit good consistency between the simulation and the vehicle test. The validation of the model basis is given, using limited data. Moreover, according to the test results, roll angles of the tractor and semitrailer shown in Figure 3(g) are very small (less than 1 deg), so vehicle roll motions on wet and slippery road could be ignored reasonably. Therefore, it can be conservatively concluded that the established 5DOF nonlinear dynamics model closely reflects the physical properties.

3. Bifurcation of Steering

Bifurcation theory is the mathematical study of changes in the qualitative or topological structure of a given family, such as the integral curves of a family of vector fields, and the solutions of a family of differential equations. Most commonly applied to the mathematical study of dynamical systems, a bifurcation occurs when a small smooth change made to the parameter values (the bifurcation parameters) of a system causes a sudden "qualitative" or topological change in its behavior. The name "bifurcation" was first introduced by Henri Poincaré in 1885 in the first paper in mathematics showing such a behavior [67, 68].

In view of the lane change handling steps, steering at a high speed on a highway under rainy weather is the primary extensive condition within the whole process. Considering the specific features of tractor-semitrailer, the vehicle nonlinear dynamics with large-scale steering on wet road are more complex than single vehicle under the normal situation and are analyzed in the following subsections.

3.1. Vehicle Model Transformation. In order to efficiently analyze tractor-semitrailer's bifurcation characteristics in typical work conditions and simplify calculation process, steering wheel is not applied as the input of steering, front wheel instead. Based on the idea, the vehicle system is transformed as

$$\dot{\mathbf{X}} = f(\mathbf{X}, \delta_f), \quad (7)$$

where $\mathbf{X} = (v_{xt}, v_{yt}, \dot{\varphi}_t, \dot{\theta}, \theta)^T$.

In the case of the vehicle steering motion, suppose the vector $\mathbf{X}^e = (v_{xt}^e, v_{yt}^e, \dot{\varphi}_t^e, \dot{\theta}^e, \theta^e)^T$ is an equilibrium point for the system described in (7). To assess the system behavior

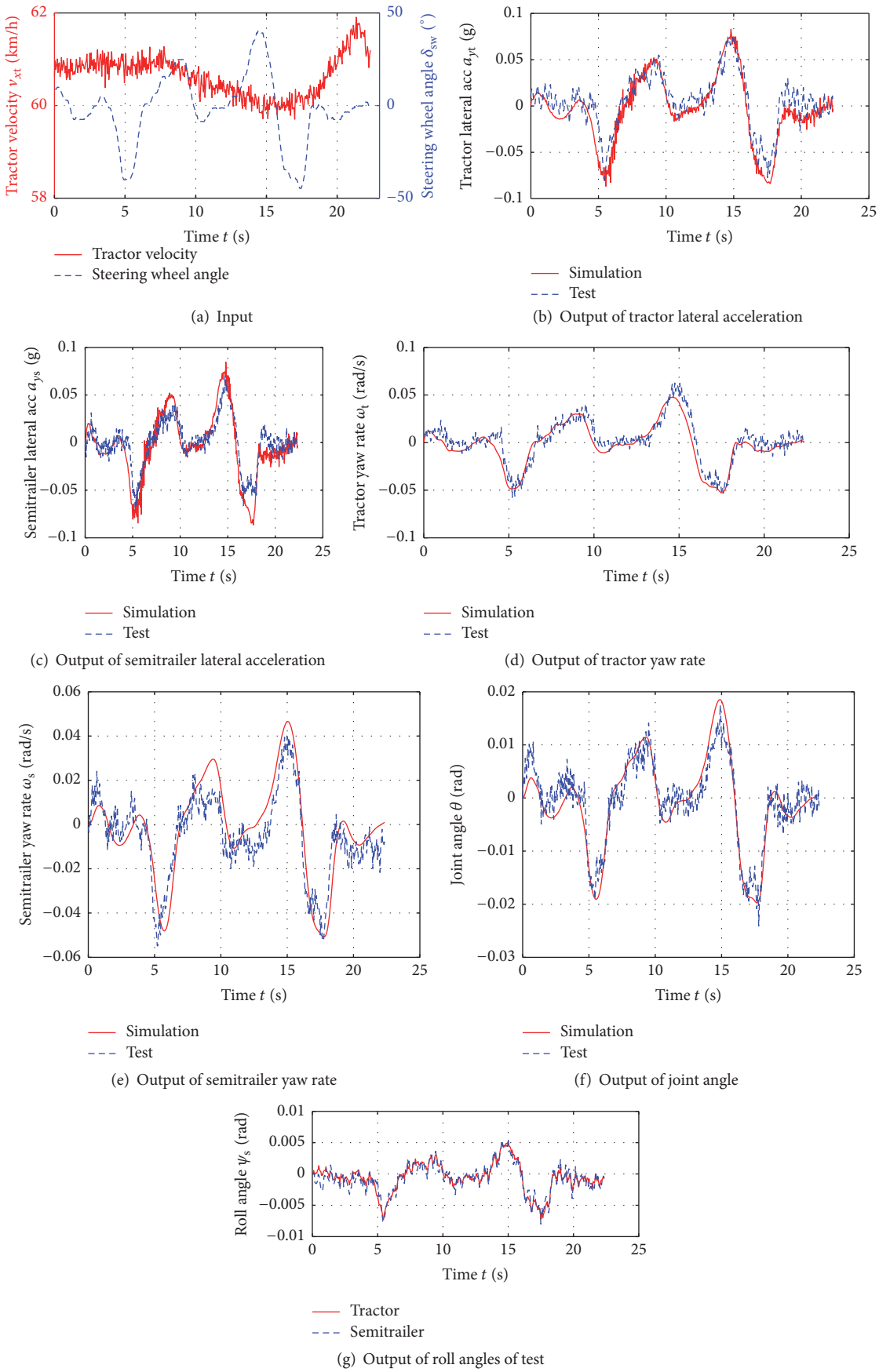

(a) Input

(b) Output of tractor lateral acceleration

(c) Output of semitrailer lateral acceleration

(d) Output of tractor yaw rate

(e) Output of semitrailer yaw rate

(f) Output of joint angle

(g) Output of roll angles of test

Figure 3: Comparison of simulation and vehicle test.

Table 3: Calculated eigenvalues of Jacobian matrix A under various front wheel steering angles.

δ_f/rad	Eig. 1		Eig. 2		Eig. 3		Eig. 4		Eig. 5	
	Re	Im	Re	Im	Re	Im	Re	Im	Re	Im
0.01	−1.8135	3.3965	−1.8135	−3.3965	−1.3298	2.1452	−1.3298	−2.1452	−0.0001	0
0.02	−1.7838	3.3517	−1.7838	−3.3517	−1.3154	2.1192	−1.3154	−2.1192	−0.0006	0
0.03	−1.7011	3.2258	−1.7011	−3.2258	−1.2801	2.0400	−1.2801	−2.0400	−0.0014	0
0.04	−1.4962	2.9357	−1.4962	−2.9357	−1.2203	1.8070	−1.2203	−1.8070	−0.0032	0
0.049	−0.8385	2.2125	−0.8385	−2.2125	0	0.1102	0	−0.1102	−2.1906	0

after stability loss, (7) is expanded into a multidimensional Taylor series in x_i around $\mathbf{X}^e$ up to order 3, yielding

$$\dot{\mathbf{X}} = A\mathbf{X} + F\left(\mathbf{X}, \delta_f\right) + \mathbf{O}\left(|\mathbf{X}|^4\right), \tag{8}$$

where A is the Jacobian matrix of the nonlinear function $f(\mathbf{X}, \delta_f)$, computed at the equilibrium point $\mathbf{X}^e$ and $F(\mathbf{X}, \delta_f)$ contains nonlinear terms of order 3 at $\mathbf{X}^e$:

$$A = D_{\mathbf{x}} f\left(\mathbf{X}, \delta_f\right)\Big|_{(v_{xt}^e, v_{yt}^e, \dot{\varphi}_t^e, \dot{\theta}^e, \theta^e)^T}. \tag{9}$$

The fifth-order characteristic equation of Jacobian matrix A is as follows:

$$\lambda^5 + c_1\lambda^4 + c_2\lambda^3 + c_3\lambda^2 + c_4\lambda + c_5 = 0. \tag{10}$$

According to Hurwitz stability criterion, if and only if all the roots of Jacobian matrix A have strictly negative real part, the system is stable. The criterion identifies the conditions when the poles of a polynomial cross into the right hand half plane and hence would be considered as unstable in control engineering [67–69].

3.2. Bifurcation of Steady Steering. Steady steering not only is a typical working condition, for exhibiting vehicle steady characteristics, but also is the basic of transient. Good steady characteristics predict better transient performance to a certain extent.

With initial longitudinal velocity 20 m/s, the calculated five eigenvalues (Re represents the real part and Im represents the imaginary part) of Jacobian matrix A with front wheel steering angle varying in the range [0.01, 0.049] rad are listed in Table 3.

As shown in Table 3, when the steering angle is less than 0.049 rad, there are five eigenvalues with negative real parts. According to the nonlinear theory, in these cases, the vehicle system is stable and the equilibrium points are called nodal points. Once the steering angle reaches 0.049 rad, two pairs of imaginary eigenvalues with zero real parts appear, which means that a Hopf bifurcation may exist [69].

According to [68], there is a pair of pure imaginary conjugate eigenvalues and the other eigenvalues have nonzero real part; thus, the corresponding equilibrium point is non-hyperbolic. In addition, it is clearly seen that the real part of the eigenvalues varies as the steering angle increases, and the transverse condition is satisfied as follows:

$$\begin{aligned}\left.\frac{d\,\mathrm{Re}\,(\lambda)}{d\delta_f}\right|_{\delta_f=0.049} &= \mathrm{Re}\left(\frac{d\,(\lambda)}{d\delta_f}\right)\Big|_{\delta_f=0.049} \\ &= \frac{0-(-1.2203)}{0.049-0.04} = 135.59 \neq 0.\end{aligned} \tag{11}$$

Therefore, it is proved that the Hopf bifurcation is taking place at the equilibrium point when $\delta_f = 0.049$ rad.

The equilibrium point could be calculated with the vehicle model by Matlab. Input parameters are $\delta_f = 0.049$ rad and initial $v_x = 20$ m/s; the system will be stable within a limited period of time; then the equilibrium point could be obtained according to the stable variables; that is, $(\mathbf{X}^e, \delta_f) = (-1.3162, 0.0761, 0, 0.0576, 19.86, 0.049)$.

Once Hopf bifurcation is taking place, under reasonably generic assumptions about the dynamical system, as steering angle slightly rises, a periodic solution called limit cycle branches from the fixed point [67, 68]. When the steering angle is 0.05 rad, limit circles of tractor's velocities with time are shown in Figure 4.

It can be seen from Figure 4, as time increases, a large-scale periodic vibration of the tractor's velocities, which represents a periodic solution of vehicle system. So there is limit circle when the steering angle is 0.05 rad, after Hopf bifurcation has taken place, which shows large range conversion of vehicle longitudinal and lateral kinetic energy. Obviously, the energy conversion could not be realized in reality because of frictional loss and motion constraint between tractor and semitrailer. However, the articulated vehicle's conservation of energy and dynamic trends of stability loss is clearly revealed.

For the 4DOF model with longitudinal velocity changes, the state variable of quasiperiodic vibration shows energy conservation. Moreover, the eigenvalues change from imaginary with negative real part to pure imaginary in accordance with the manifolds, predicting the Hopf bifurcation phenomenon. It is verified that a pair of conjugate roots, first crossing on the imaginary axis, translates into oscillatory behavior leading to instability.

3.3. Bifurcation of Sinusoidal Steering. Sinusoidal steering is introduced to approximately represent the steering process for lane changing. Unlike steady steering, the front wheel steering angle is represented as

$$\delta_f = A_s \sin\left(2\pi f t\right), \tag{12}$$

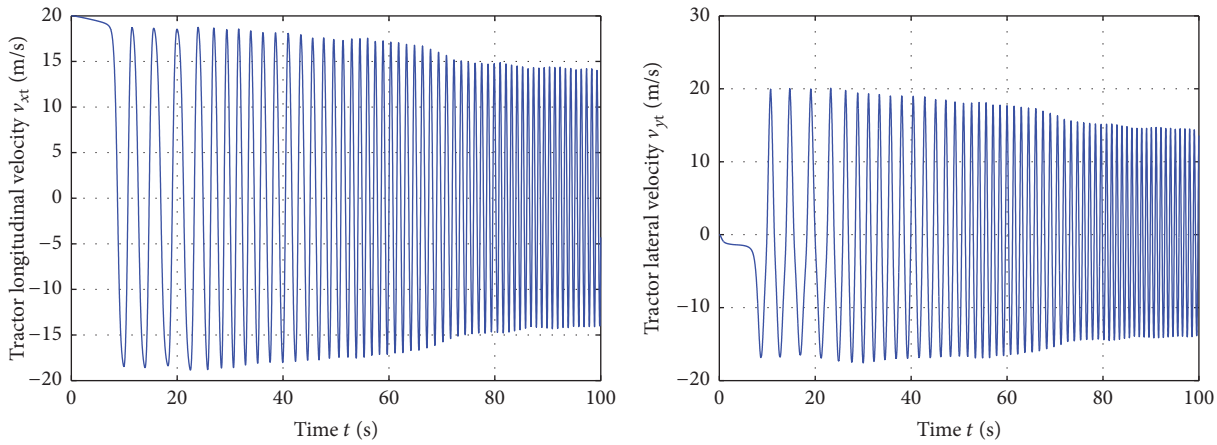

(a) Tractor longitudinal velocity

(b) Tractor lateral velocity

Figure 4: Limit circle of tractor's velocities with $\delta_f = 0.05$ rad.

where A_s is the steering amplitude and f is steering frequency. Compared with steady steering, the vehicle with sinusoidal steering is considered a time-changing system. The equilibrium points and corresponding eigenvalues vary with time and the steering angle.

Figure 5 shows the changes in the steering angle, lateral velocity, and calculated eigenvalues when the initial longitudinal velocity is 20 m/s, and the front wheel steering amplitude and frequency are, respectively, 0.06 rad and 0.2 Hz. With $A_s = 0.06$ rad, $f = 0.2$ Hz, the calculated eigenvalues present a double wave shape with sinusoidal steering. According to the tractor lateral velocity, the vehicle system is still stable, although transit values of eigenvalue 1 and eigenvalue 3 are positive or have positive real parts during steering. In addition, when $t > 6.3$ s, all of the eigenvalues are negative as steer returning takes place and eigenvalue 5 is approximately equal to 0. Therefore, it can be concluded that the negative eigenvalue is sufficient, but not necessary, for judging stability. Furthermore, comparing sinusoidal and steady steering, when the front wheel angle is greater than 0.05 rad, the vehicle system with steady steering loses stability, but that with sinusoidal steering remains stable. Specifically, vehicle stability is influenced by the frequency and the transient state.

Figure 6 shows, as the amplitude is increased from 0.06 rad to 0.07 rad, the changes in the steering angle, lateral velocity, and calculated eigenvalues.

It can be seen from Figure 6 that, as the steering amplitude increases to 0.07 rad, not only transit values of eigenvalue 1 and eigenvalue 3 are positive or have positive real parts during steering, just as $A_s = 0.06$ rad, but also transit values of eigenvalue 5 are positive eigenvalues after steer returning. Meanwhile, there is a pair of conjugate eigenvalues (eigenvalues 1 and 2), approximately lying on the imaginary axis, which indicates the existence of Hopf bifurcation. Figure 7 shows the unstable limit circle of the vehicle typical parameters with continuous sinusoidal steering when $A_s = 0.07$ rad, $f = 0.2$ Hz.

Just as in Figure 4 for the case of steady steering, Figure 7 shows an unstable limit circle of vehicle dynamic motions with critical sinusoidal steering. It clearly shows there are obvious differences in fluctuation range of vehicle's lateral velocity between steady and sinusoidal steering. Besides this, the vehicle's dynamic bifurcation and oscillatory behavior are identical.

4. Bifurcation Control with Feedback Linearization

It is obvious that, with the Jacobian matrix A induced by vehicle's nonlinear model, the eigenvalues could reveal the bifurcation characteristics and stability. Thus, basic ideal is proposed to ensure the eigenvalues with negative real parts, by proper control method.

Feedback Linearization is an approach to nonlinear control design which has attracted a great deal of research interest in recent years. Algebraically transform a nonlinear system into a (fully or partly) linear one, so that linear control techniques can be applied. *This differs from the conventional linearization in that feedback linearization is achieved by exact state transformations and feedback, rather than by linear approximations of the dynamics [63, 69–72].* Considering the nonlinearity of tractor-semitrailer, based on feedback linearization theory, an integrated controller is introduced to realize vehicle system asymptotically stable and tracking performance in this section.

4.1. Vehicle Control Model. Supposing the tractor longitudinal velocity constant, the vehicle model introduced in Section 2 is deduced as follows:

$$\dot{\mathbf{X}} = f\left(\mathbf{X}, \delta_{sw}\right), \tag{13}$$

where $\mathbf{X} = [x_1, x_2, x_3, x_4, x_5, x_6]^T = [v_{yt}, \dot{\varphi}_t, \dot{\theta}, \theta, \dot{\delta}_f, \delta_f]^T$.

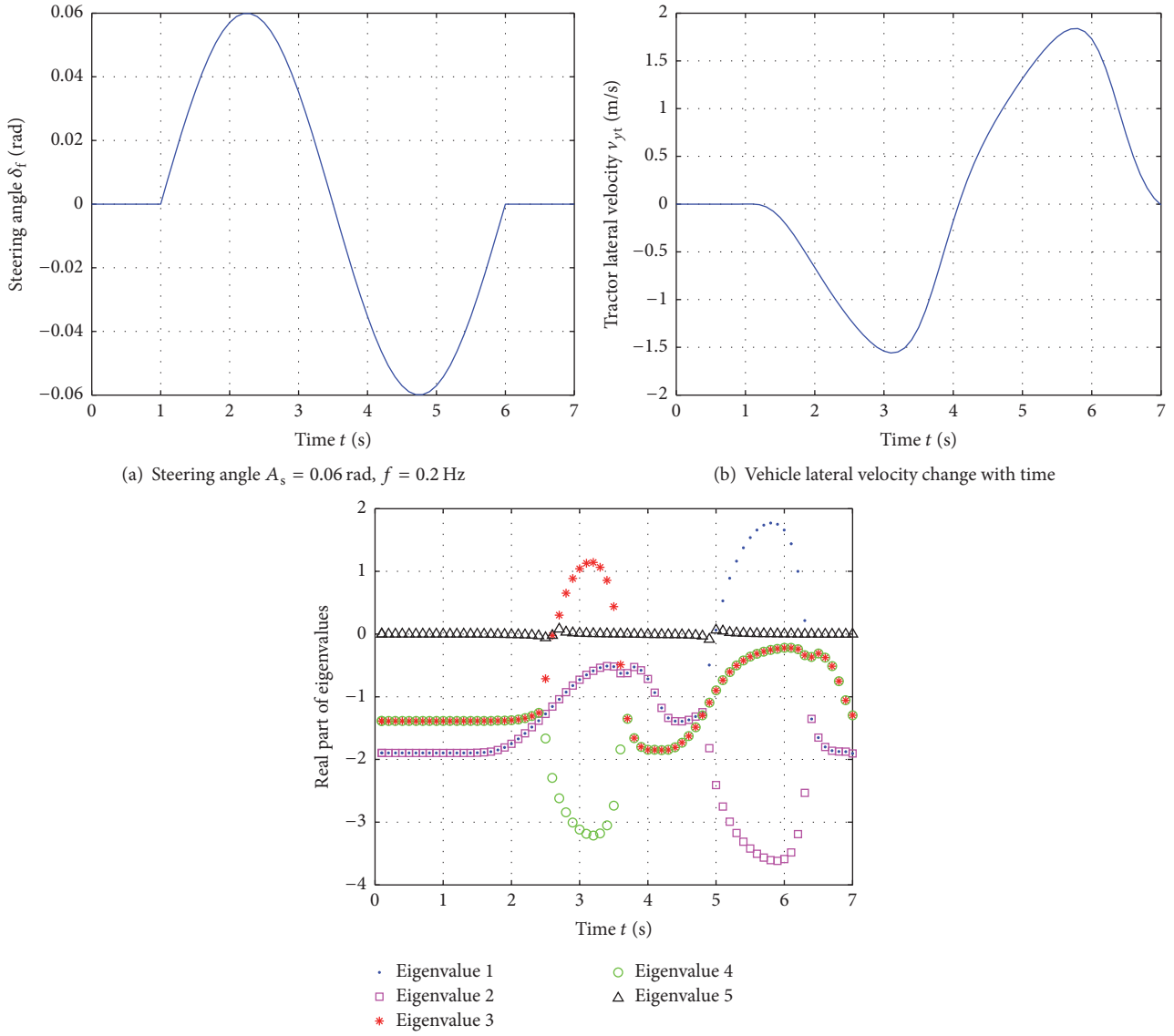

(a) Steering angle $A_s = 0.06$ rad, $f = 0.2$ Hz

(b) Vehicle lateral velocity change with time

(c) Real part of eigenvalues change with time

FIGURE 5: Changes in steering angle, lateral velocity, and calculated eigenvalues with $A_s = 0.06$ rad, $f = 0.2$ Hz.

In order to linearize nonlinear systems by feedback linearization method, feedback parameters, as control outputs, not only are controllable, but also ensure linearization. Therefore, setting tractor yaw rate $\dot{\varphi}_t$ and the difference of joint angle and steering angle $\theta - \delta_f$ as control output variables, applying AFS and DYC combined control method, the feedback linearization control model could be described as

$$\begin{aligned} \dot{\mathbf{X}} &= f(\mathbf{X}, \delta_{sw}) + g_1 u_1 + g_2 u_2, \\ y_1 &= h_1(x) = \dot{\varphi}_t, \\ y_2 &= h_2(x) = \theta - \delta_f, \end{aligned} \tag{14}$$

where

$$f(\mathbf{X}, \delta_{sw}) = \begin{bmatrix} a_{11}F_{yf} + a_{12}F_{yr} + a_{13}F_{ys} + a_{14}v_{xt}x_2 \\ a_{21}F_{yf} + a_{22}F_{yr} + a_{23}F_{ys} \\ a_{31}F_{yf} + a_{32}F_{yr} + a_{33}F_{ys} \\ x_3 \\ -\dfrac{C_w x_5}{I_w} - \dfrac{K_w x_6}{I_w} - \dfrac{\varepsilon F_{ytf}}{I_w} + \dfrac{K_w}{iI_w}\delta_{sw} \\ x_5 \end{bmatrix}, \tag{15}$$

$$\begin{aligned} g_1 &= \left[0, 0, 0, 0, -\frac{K_w}{I_w}, 0\right]^T, \\ g_2 &= [g_{21}, g_{22}, g_{23}, 0, 0, 0]^T, \end{aligned} \tag{16}$$

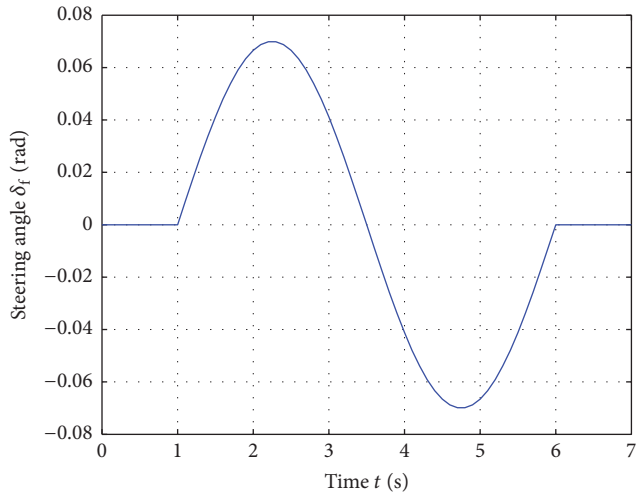

(a) Steering angle $A_s = 0.06$ rad, $f = 0.2$ Hz

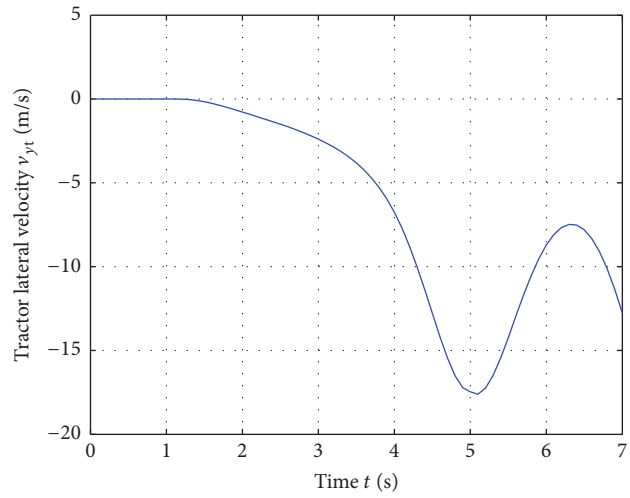

(b) Vehicle lateral velocity change with time

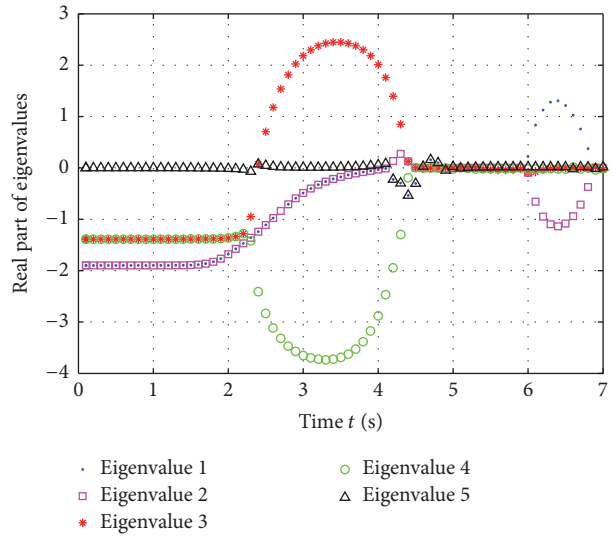

(c) Real part of eigenvalues change with time

FIGURE 6: Changes in steering angle, lateral velocity, and real parts of calculated eigenvalues with $A_s = 0.07$ rad, $f = 0.2$ Hz.

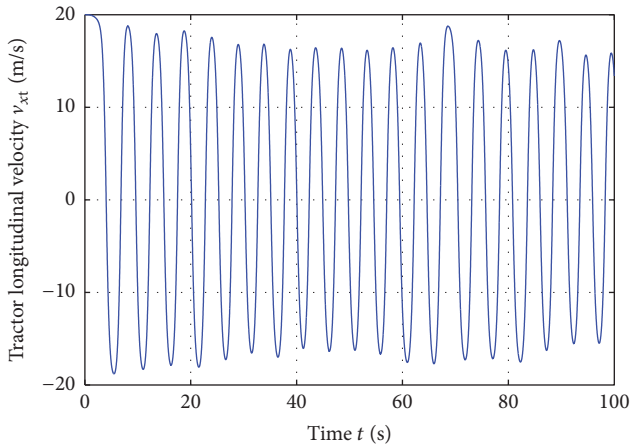

(a) Tractor longitudinal velocity

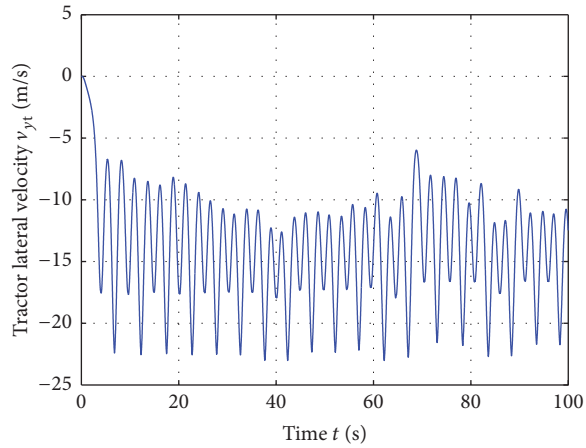

(b) Tractor lateral velocity

FIGURE 7: Limit circle of vehicle's velocity with $A_s = 0.07$ rad, $f = 0.2$ Hz.

$$u_1 = \delta_{\mathrm{swc}},$$
$$u_2 = M_{\mathrm{c}}. \tag{17}$$

Variables a_{11}, a_{12}, a_{13}, and so on in (15) and g_{21}, g_{22}, and g_{23} in (16) could be expressed by known variables, as follows:

$$a_{11} = \frac{(a_1 + c)\, cm_2 I_{z2} + I_{z1} I_{z2} + a_2^2 m_2 I_{z1}}{S},$$
$$a_{12} = \frac{(c - b_1)\, cm_2 I_{z2} + I_{z1} I_{z2} + a_2^2 m_2 I_{z1}}{S},$$
$$a_{13} = \frac{(I_{z2} - a_2 b_2 m_2)\, I_{z1}}{S},$$
$$a_{14} = \frac{-\left(a_2^2 I_{z1} + c^2 I_{z2}\right) m_1 m_2 - (m_1 + m_2)\, I_{z1} I_{z2}}{S},$$
$$a_{21} = \frac{a_1 a_2^2 m_1 m_2 + (a_1 m_1 + a_1 m_2 + cm_2)\, I_{z2} - a_2 m_2 I_{z1}}{S},$$
$$a_{22} = \frac{(cm_2 - b_1 m_1 - b_1 m_2)\, I_{z2} - a_2^2 b_1 m_1 m_2}{S},$$
$$a_{23} = \frac{cm_1 (a_2 b_2 m_2 - I_{z2})}{S},$$
$$a_{31} = \frac{a_1 a_2 (c + a_2)\, m_1 m_2 + (a_1 m_1 + a_1 m_2 + cm_2)\, I_{z2} - a_2 m_2 I_{z1}}{S},$$
$$a_{32} = \frac{-a_2 b_1 (c + a_2)\, m_1 m_2 + (cm_2 - b_1 m_2 - b_1 m_1)\, I_{z2} - a_2 m_2 I_{z1}}{S},$$
$$a_{33} = \frac{(a_2 I_{z1} - cI_{z2})\, m_1 + b_2 \left[(m_1 + m_2)\, I_{z1} + c\,(c + a_2)\, m_1 m_2\right]}{S},$$
$$g_{21} = \frac{(a_2 I_{z1} - cI_{z2})\, m_2}{S},$$
$$g_{22} = \frac{-(a_2 + c)\, a_2 m_1 m_2 - (m_1 + m_2)\, I_{z2}}{S},$$
$$g_{23} = \frac{-(a_2 + c)^2\, m_1 m_2 - (m_1 + m_2)\, (I_{z1} + I_{z2})}{S},$$
$$S = \left(a_2^2 I_{z1} + c^2 I_{z2}\right) m_1 m_2 + (m_1 + m_2)\, I_{z1} I_{z2}. \tag{18}$$

According to conditions of feedback linearization theory, relative degree of vehicle system should be confirmed as

$$L_{g1} h_1(x) = \frac{\partial (x_2)}{\partial (\mathbf{X})} \cdot g_1 = 0;$$
$$L_{g2} h_2(x) = \frac{\partial (x_2)}{\partial (\mathbf{X})} \cdot g_2 = g_{22} \neq 0;$$
$$L_{g1} h_2(x) = \frac{\partial (x_4 - x_6)}{\partial (\mathbf{X})} \cdot g_1 = 0;$$
$$L_{g2} h_2(x) = \frac{\partial (x_4 - x_6)}{\partial (\mathbf{X})} \cdot g_2 = 0;$$
$$L_f h_1(x) = \frac{\partial (x_2)}{\partial (\mathbf{X})} \cdot f(\mathbf{X}) = a_{21} F_{y\mathrm{tf}} + a_{22} F_{y\mathrm{tr}} + a_{23} F_{y\mathrm{s}};$$
$$L_f h_2(x) = \frac{\partial (x_4 - x_6)}{\partial (\mathbf{X})} \cdot f(\mathbf{X}) = x_3 - x_5;$$
$$L_{g1} L_f h_2(x) = \frac{\partial (x_3 - x_5)}{\partial (\mathbf{X})} \cdot g_1 = \frac{k_{\mathrm{w}}}{I_{\mathrm{w}}} \neq 0;$$
$$L_{g2} L_f h_2(x) = \frac{\partial (x_3 - x_5)}{\partial (\mathbf{X})} \cdot g_2 = g_{23} \neq 0;$$
$$L_f^2 h_2(x) = \frac{\partial (x_3 - x_5)}{\partial (\mathbf{X})} \cdot f(\mathbf{X}) = \left(a_{31} + \frac{\varepsilon}{I_{\mathrm{w}}}\right) F_{y\mathrm{tf}} + a_{32} F_{y\mathrm{tr}} + a_{33} F_{y\mathrm{s}} + \frac{C_{\mathrm{w}}}{I_{\mathrm{w}}} x_5 + \frac{k_{\mathrm{w}}}{I_{\mathrm{w}}} x_6 - \frac{k_{\mathrm{w}}}{I_{\mathrm{w}}} \delta_{\mathrm{sw}}. \tag{19}$$

It is concluded that relative degree of vehicle system is 3 less than 6, which satisfies partial feedback linearization.

Coordinate transformation is necessary for the model, as

$$\mathbf{Z} = [z_1, z_2, z_3, z_4, z_5, z_6]^{\mathrm{T}} = \left[x_2, x_4 - x_6, x_3 - x_5, -\frac{g_{22} x_1}{g_{21}} + x_2, -\frac{g_{23} x_1}{g_{21}} + x_3, x_6\right],$$
$$\mathbf{X} = [x_1, x_2, x_3, x_4, x_5, x_6]^{\mathrm{T}} = \left[\frac{g_{21}(z_1 - z_4)}{g_{22}}, z_1, z_5 + \frac{g_{21}(z_1 - z_4)}{g_{22}}, z_2 + z_6, z_5 - z_3 + \frac{g_{23}(z_1 - z_4)}{g_{22}}, z_6\right]^{\mathrm{T}}. \tag{20}$$

Then, partial feedback linearization control model is as follows:

$$\dot{\boldsymbol{\xi}} = A_{\mathrm{c}} \boldsymbol{\xi} + B_{\mathrm{c}} \gamma(\mathbf{X}) [\mathbf{u} - \alpha(\mathbf{X})],$$
$$\dot{\boldsymbol{\eta}} = q_0(\boldsymbol{\eta}, \boldsymbol{\xi}),$$
$$\mathbf{y} = C_{\mathrm{c}} \boldsymbol{\xi}, \tag{21}$$

where $\boldsymbol{\xi} = [z_1, z_2, z_3]^{\mathrm{T}}$; $\boldsymbol{\eta} = [z_4, z_5, z_6]^{\mathrm{T}}$.

That is,

$$\dot{\boldsymbol{\xi}} = \begin{bmatrix} \dot{z}_1 \\ \dot{z}_2 \\ \dot{z}_3 \end{bmatrix} = \begin{bmatrix} 0 & 0 & 0 \\ 0 & 0 & 1 \\ 0 & 0 & 0 \end{bmatrix} \begin{bmatrix} z_1 \\ z_2 \\ z_3 \end{bmatrix} + \begin{bmatrix} L_f h_1(x) + L_{g1} h_1(x) u_1 + L_{g2} h_2(x) u_2 \\ 0 \\ L_f^2 h_2(x) + L_{g1} L_f h_2(x) u_1 + L_{g2} L_f h_2(x) u_2 \end{bmatrix},$$

$$\dot{\boldsymbol{\eta}} = \begin{bmatrix} \dot{z}_4 \\ \dot{z}_5 \\ \dot{z}_6 \end{bmatrix} = \begin{bmatrix} \left(a_{21} - \frac{g_{22}a_{11}}{g_{21}}\right) F_{ytf} + \left(a_{22} - \frac{g_{22}a_{12}}{g_{21}}\right) F_{ytr} + \left(a_{23} - \frac{g_{22}a_{13}}{g_{21}}\right) F_{ys} - \frac{g_{22}a_{14}x_2}{g_{21}} \\ \left(a_{31} - \frac{g_{23}a_{11}}{g_{21}}\right) F_{ytf} + \left(a_{32} - \frac{g_{23}a_{12}}{g_{21}}\right) F_{ytr} + \left(a_{33} - \frac{g_{23}a_{13}}{g_{21}}\right) F_{ys} - \frac{g_{23}a_{14}x_2}{g_{21}} \\ x_5 \end{bmatrix}, \tag{22}$$

$$\mathbf{y} = \begin{bmatrix} 1 & 0 & 0 \\ 0 & 1 & 0 \\ 0 & 0 & 0 \end{bmatrix} \begin{bmatrix} z_1 \\ z_2 \\ z_3 \end{bmatrix}.$$

According to (14) and (22), it is satisfied that $x_2 = x_3 = x_4 = x_5 = x_6 = 0$ if $\boldsymbol{\xi} = [z_1, z_2, z_3] \equiv 0$. Thus, the zero dynamic equation $\dot{\boldsymbol{\eta}} = [\dot{z}_4, \dot{z}_5, \dot{z}_6]^{\mathrm{T}}$ is asymptotic stable at the origin. So it is proved that the vehicle feedback linearization model could be effectively controlled by $\dot{\boldsymbol{\xi}} = [\dot{z}_1, \dot{z}_2, \dot{z}_3]^{\mathrm{T}}$.

Defining control input variable $\mathbf{v}$, as

$$\begin{aligned} \mathbf{v} &= \begin{bmatrix} v_1 \\ v_2 \end{bmatrix} \\ &= \begin{bmatrix} L_f h_1(x) + L_{g1} h_1(x) u_1 + L_{g2} h_1(x) u_2 \\ L_f^2 h_2(x) + L_{g1} L_f h_2(x) u_1 + L_{g2} L_f h_2(x) u_2 \end{bmatrix}, \end{aligned} \tag{23}$$

then initial system could be transformed as a linear system $\dot{\boldsymbol{\xi}} = A_c \boldsymbol{\xi} + B_c \mathbf{v}$.

4.2. Feedback Linearization Controller Design. A linear 4DOF model of tractor-semitrailer is introduced to obtain a reference for control output. Just as the controlled model (13), the reference 4DOF vehicle model also considers tractor and semitrailer's lateral motions and yaw motions and steering wheel rotation. The only difference is that it is applied linear tire model, as

$$F_y = k\alpha, \tag{24}$$

where k is tire slip stiffness and α is tire slip angle.

Based on first-order Taylor expansion of magic formula (5), k of each tractor-semitrailer's tire could be calculated by $k_i = B_i C_i D_i$, whose values are shown in Table 2.

The reference 4DOF vehicle model is describes as

$$\dot{\mathbf{X}}_{\mathrm{r}} = A_{\mathrm{r}} \mathbf{X}_{\mathrm{r}} + B_{\mathrm{r}} \delta_{\mathrm{sw}}, \tag{25}$$

where the reference state variables $\mathbf{X}_{\mathrm{r}} = [x_{1\mathrm{r}}, x_{2\mathrm{r}}, x_{3\mathrm{r}}, x_{4\mathrm{r}}, x_{5\mathrm{r}}, x_{6\mathrm{r}}]^{\mathrm{T}} = [v_{y\mathrm{tr}}, \dot{\varphi}_{\mathrm{tr}}, \dot{\theta}_{\mathrm{r}}, \theta_{\mathrm{r}}, \dot{\delta}_{\mathrm{fr}}, \delta_{\mathrm{fr}}]^{\mathrm{T}}$ and the reference outputs are $y_{1\mathrm{r}} = x_{1\mathrm{r}}$ and $y_{2\mathrm{r}} = x_{4\mathrm{r}} - x_{6\mathrm{r}}$. A_{r} and B_{r} are as follows:

$$A_{\mathrm{r}} = \begin{bmatrix} m_{\mathrm{t}} + m_{\mathrm{s}} & -(c + a_{\mathrm{s}}) m_{\mathrm{s}} & a_{\mathrm{s}} m_{\mathrm{s}} & 0 & 0 & 0 \\ c m_{\mathrm{t}} & I_{zt} & 0 & 0 & 0 & 0 \\ a_{\mathrm{s}} m_{\mathrm{t}} & I_{zs} & -I_{zs} & 0 & 0 & 0 \\ 0 & 0 & 0 & 1 & 0 & 0 \\ 0 & 0 & 0 & 0 & I_{\mathrm{w}} & 0 \\ 0 & 0 & 0 & 0 & 0 & 1 \end{bmatrix}^{-1}$$

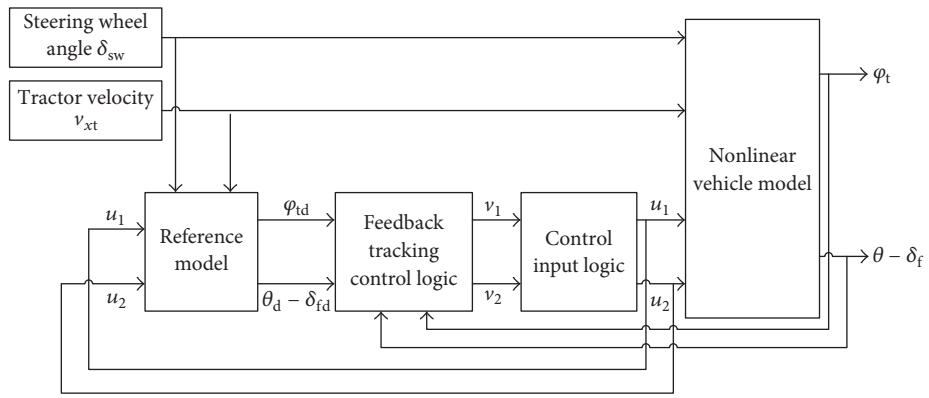

Figure 8: Structure of feedback tracking controller.

$$\times \begin{bmatrix} k_{tf}+k_{tr}+k_s & -\left[(m_s+m_t)v_{xt} - \dfrac{a_t k_{tf} - b_t k_{tr} - (c+a_s+b_s)k_s}{v_{xt}}\right] & \dfrac{(a_s+b_s)k_s}{v_{xt}} & k_s & 0 & -k_{tf} \\ (a_t+c)k_{tf} + (c-b_t)k_{tr} & -cm_t v_{xt} + \dfrac{a_t(a_t+c)k_{tf} + b_t(b_t-c)k_{tr}}{v_{xt}} & 0 & 0 & 0 & -(a_t+c)k_{tf} \\ a_s(k_{tf}+k_{tr}) - b_s k_s & -a_s m_t v_{xt} + \dfrac{a_s(a_t k_{tf} - b_t k_{tr}) + b_s(c+a_s+b_s)k_s}{v_{xt}} & -\dfrac{b_s(a_s+b_s)k_s}{v_{xt}} & -b_s k_s & 0 & -a_s k_{tf} \\ 0 & 0 & 1 & 0 & 0 & 0 \\ -\dfrac{\varepsilon k_{tf}}{v_{xt}} & -\dfrac{a_t \varepsilon k_{tf}}{v_{xt}} & 0 & 0 & -C_w & \varepsilon k_{tf} - K_w \\ 0 & 0 & 0 & 0 & 1 & 0 \end{bmatrix},$$

$$B_r = \begin{bmatrix} 0 & 0 & 0 & 0 & \dfrac{K_w}{i} & 0 \end{bmatrix}. \tag{26}$$

Figure 8 shows a designed feedback tracking controller. The control input variable $\mathbf{v}$ is defined as

$$\begin{aligned} v_1 &= -\lambda_1 e_1 + \dot{y}_{1r}, \\ v_2 &= -\lambda_2 e_2 - \lambda_3 \dot{e}_2 + \ddot{y}_{2r}, \end{aligned} \tag{27}$$

where e_1 and e_2 are tracking errors, $e_1 = y_1 - y_{1r}$ and $e_2 = y_2 - y_{2r}$.

Equation (27) is satisfied as

$$\begin{aligned} \dot{e}_1 + \lambda_1 e_1 &= 0, \\ \ddot{e}_2 + \lambda_3 \dot{e}_2 + \lambda_2 e &= 0. \end{aligned} \tag{28}$$

Therefore, the closed-loop system errors e_1 and e_2 are exponentially stable by reasonable choice of λ_1, λ_2, and λ_3.

4.3. Control Performance Analysis. The specific control effects are mainly considered by the control stability, rapidity, and accuracy. Typical effect parameters contain peak time t_p, overshoot $\sigma\%$, and regulation time t_s.

Applying the proposed vehicle dynamic model, driving circles of step steering and single-lane changing with 20 m/s are conducted to simulate tractor-semitrailer lane changing on highway under rainy weather.

Step steering is used to select control parameters λ_1, λ_2, and λ_3 by contrasting control effects. Choosing 4 sets of data of λ_1, λ_2, and λ_3 control effects of each set and are shown in Figure 9.

It can be seen from Figure 9 that there are slight difference among 4 sets of data. Then, maximum values of e_1, e_2, typical effect parameters t_p, $\sigma\%$, and t_s and DYC torque input are, respectively, calculated, as listed in Table 4.

Table 4 indicates the influence of control parameters for vehicle system control response and accuracy. It clearly showed some diametrically opposed change trend of control effects, such as e_1 and e_2 and $\sigma\%$ and t_s. In consideration of response time, control input size, and system stability, when $\lambda_1 = 300$, $\lambda_2 = 5000$, and $\lambda_3 = 6$, values of the peak time $t_p = 1.08$ s and regulation time $t_s = 2.08$ s are all smaller, and the DYC torque input $T_{max} = 779.4590$ N is also lower correspondingly. Because of the balance of control effects, Group 2 is determined to be as final control parameters.

Based on the selected control parameters, critical scenarios of steady steering ($\delta_f = 0.05$) and single-lane changing

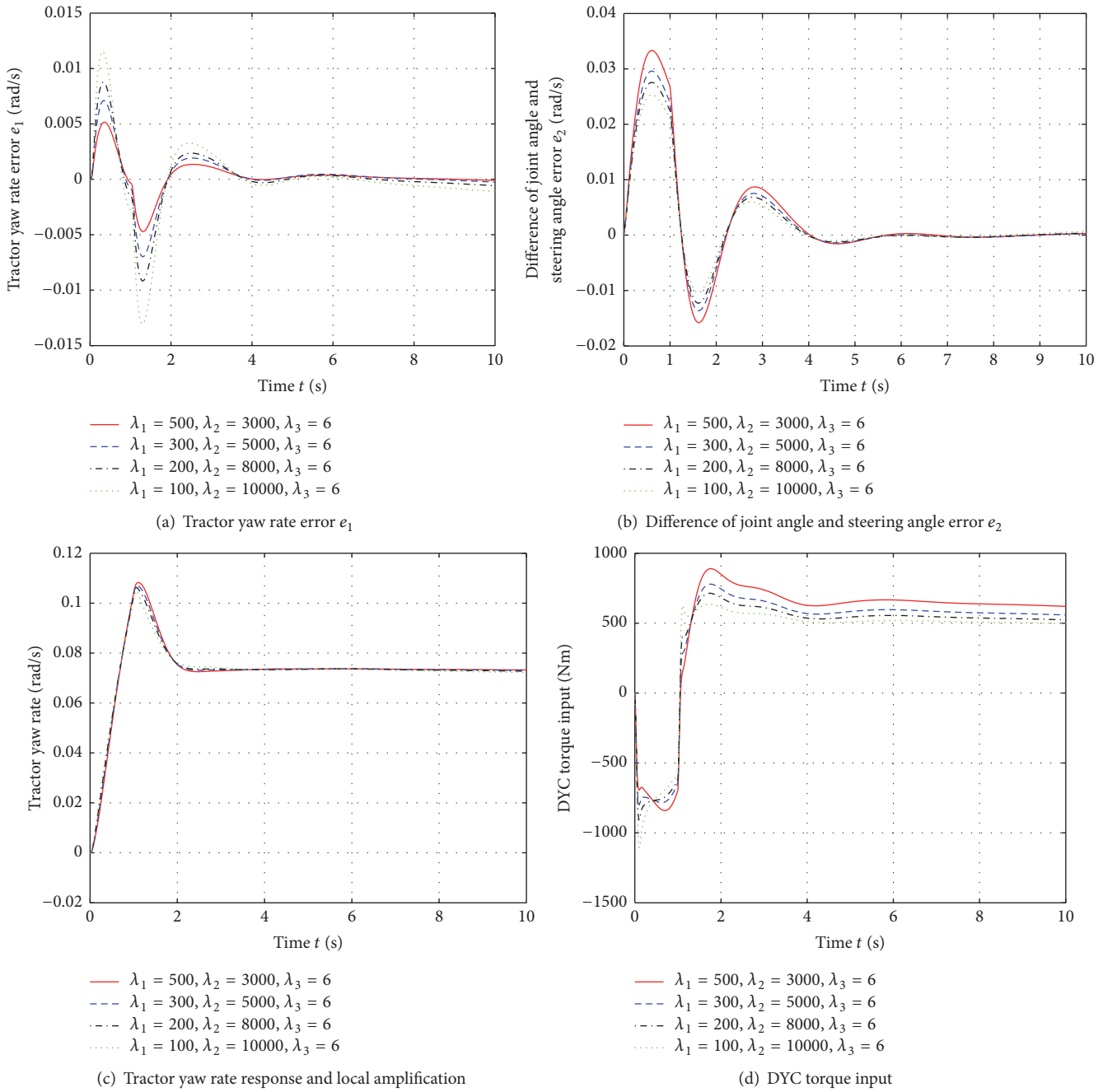

Figure 9: Control effects with 4 sets of data.

Table 4: Calculated controlled effect parameters and DYC input torques with 4 sets of data.

No.	λ_1	λ_2	λ_3	e_{1max}/rad/s	e_{2max}/rad	Tractor yaw rate response			DYC T_{max}/N
						t_p/s	σ%	t_s/s	
(1)	500	3000	6	0.0052	0.0303	1.11	47.77	2.04	809.0810
(2)	300	5000	6	0.0071	0.0296	1.08	46.59	2.08	779.4590
(3)	200	8000	6	0.0088	0.0290	1.07	46.02	2.16	751.6507
(4)	100	10000	6	0.0115	0.0281	1.06	45.26	3.34	1.2294e + 003

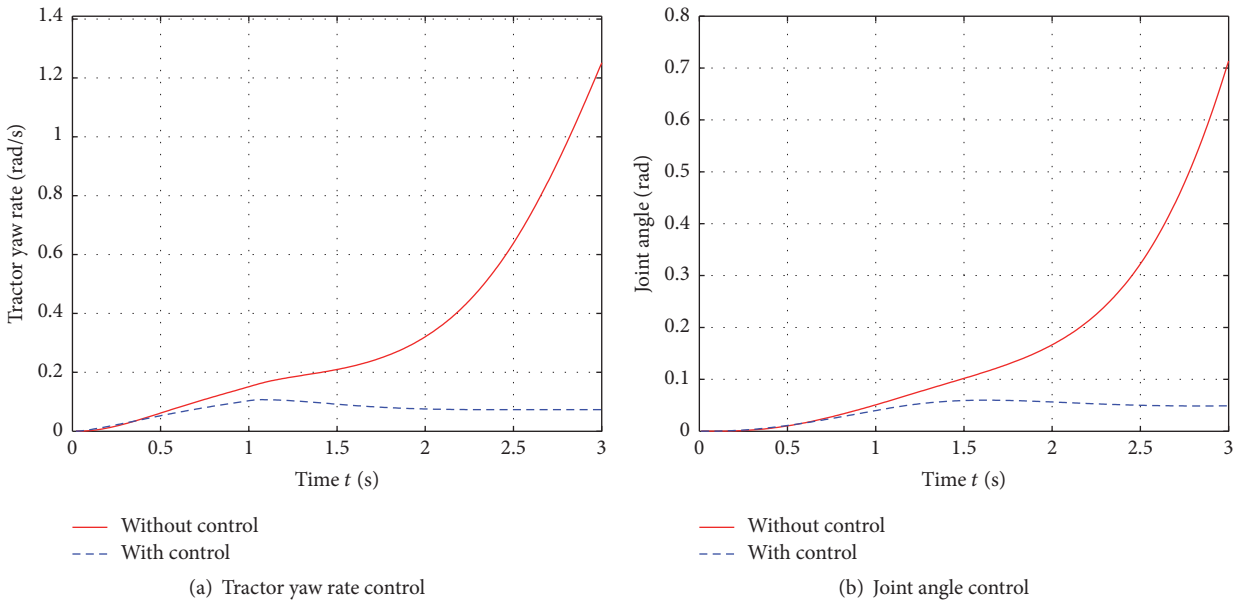

(a) Tractor yaw rate control

(b) Joint angle control

FIGURE 10: Typical contract of vehicle dynamic variables in critical steady steering.

(A_s = 0.07 rad, f = 0.2 Hz), just as introduced in Section 3, are simulated with the established feedback linearization controller. Typical contract of vehicle dynamic variables is shown in Figures 10 and 11.

Figures 10 and 11 clearly show the control effects in critical steady steering and single-lane changing conditions. It can be seen from Figure 10 that if it is without control, tractor and semitrailer yaw motions increase sharply and joint angle will reach to 0.7 rad (about 40.1 deg) in 3 seconds, which indicates that there is jackknife instability in critical steady steering. But vehicle will reach to an ideal steady state value with steady steering if applying the designed controller. Similarly, in Figure 11, vehicle dynamics is stable and the yaw motions change regularly with control in critical single-lane changing, but if it is without control, it is also obvious that the vehicles yaw sharply as yaw rate and joint angle increase rapidly (tractor yaw rate reaches about 2 rad/s in 5 seconds and joint angle reaches about 150 deg), which indicates serious sideslip and jackknife instability.

Looking back at Hopf bifurcation phenomenon and instability in critical steady steering or single-lane changing, it can be seen from Figures 10 and 11 that, by feedback linearization controller, combined with AFS and DYC strategy, vehicle's dynamic characteristics could be effectively controlled and ensure stability. In Figure 12, taking the critical single-lane changing as an example, real parts of calculated eigenvalues with control are all lying in the negative half plane with A_s = 0.07 rad, f = 0.2 Hz, which indicates the control effects in eliminating bifurcation and ensure stability.

5. Discussion and Conclusion

In this paper, considering the high degree of danger and complex maneuvers for tractor-semitrailer on low adhesion coefficient road, the nonlinear lane changing behaviors on highways under rainy weather have been studied with a verified 5DOF mechanical model based on a test experiment, and a feedback linearization controller by DYC and AFS strategy is designed to ensure stability in critical scenarios. Points of discussion and conclusions can be summarized as follows:

(1) Nonlinear theory is used to analyze the relationship between the eigenvalues of the Jacobian matrix and vehicle stability. Considering the transient response, the eigenvalues of Jacobian matrix may be positive or have positive real parts as steering wheel angle approaches peak, but the vehicle system is still stable with the angle returns. Therefore, unlike steady steering, transient stability is satisfied if there are transient positive real parts eigenvalues, so it is definitely improved that eigenvalues lying in the negative half plane is sufficient but not necessary for judging stability. It is also clearly concluded that Hopf bifurcation occurs with critical steady and sinusoidal steering, which translates into an oscillatory behavior leading to instability.

(2) It is realized for application feedback linearization theory in tractor-semitrailer stability control. Design process of an integrated controller is detailed presented with vehicle mechanical model, which contains model building, feedback linearization, and control parameters selection. The consequences of performance analysis introduce new insight into the vehicle nonlinear stability control. The eigenvalues analysis results also provide a substantive understanding on control principle.

(3) Through analyzing the vehicle nonlinear stability in special driving conditions, the dynamic rule and stability mechanism for tractor-semitrailers changing

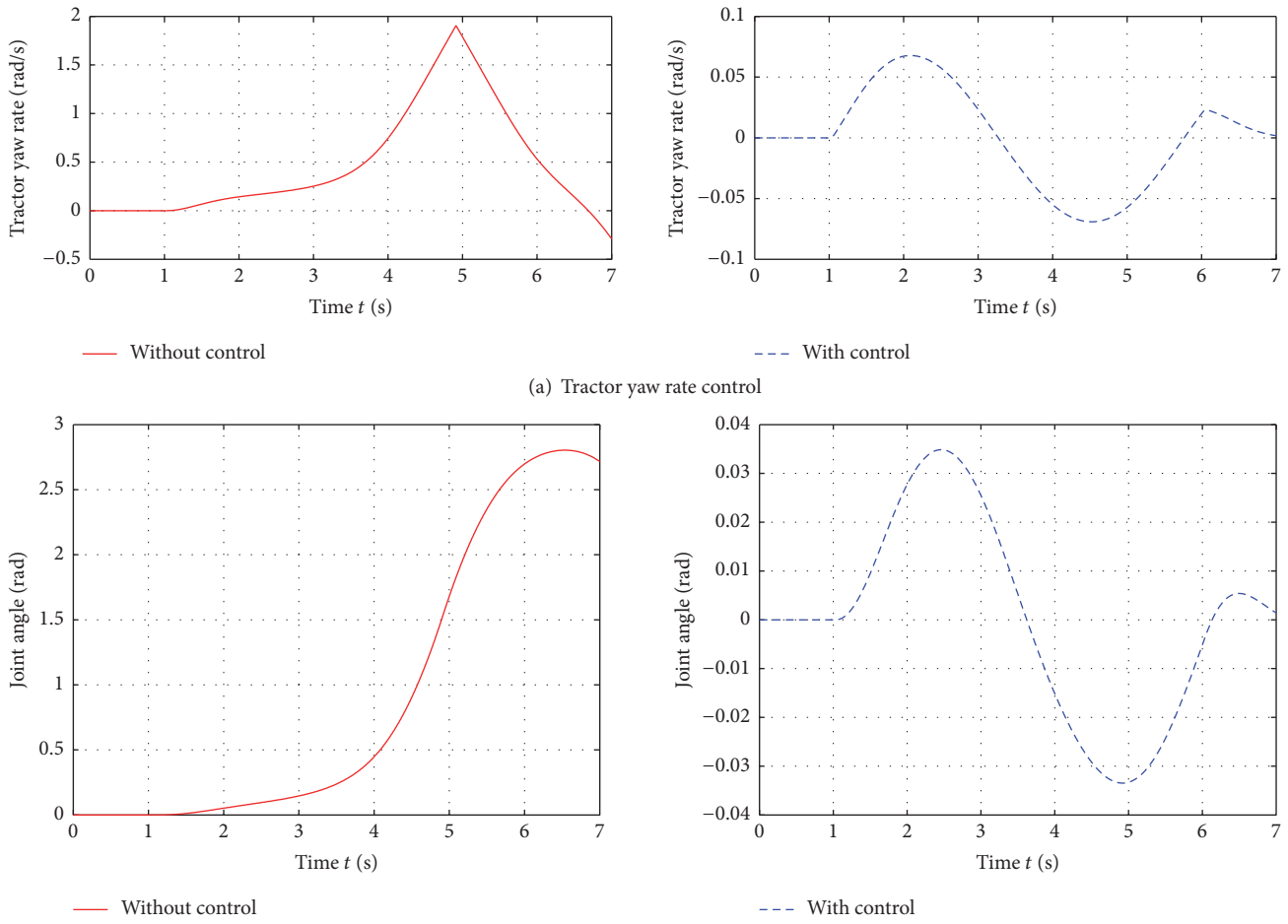

(a) Tractor yaw rate control

(b) Joint angle control

Figure 11: Typical contract of vehicle dynamic variables in critical single-lane changing.

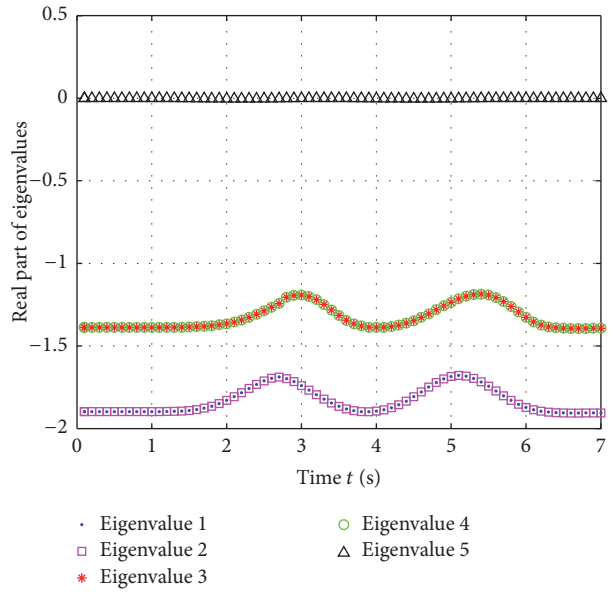

Figure 12: Changes in real parts of calculated eigenvalues with control in critical single-lane changing.

lanes at high speeds under rainy weather are well mastered. The bifurcation analysis and nonlinear control provided could be informative for research into vehicle dynamics and active safety control design.

Furthermore, tractor-semitrailers have complex nonlinear behaviors, especially considering driver and environment characteristics. The following could be considered in the future:

(1) The driver is always an early decision-maker for vehicle movement; it is essential to study the lane-changing nonlinear behaviors of tractor-semitrailers associated with driver characteristics.

(2) As the study on adhesion coefficient caused by rainy weather, the influence of the other meteorological effects, such as rain for driver sight distance and high winds for vehicle dynamic, should be taken into account to comprehensively analyze the driving stability of tractor-semitrailers.

(3) Synergetic thought should be introduced creatively to tractor-semitrailers, not only for single tractor and

semitrailer internal relationship, but also for cooperative operation management of a dynamic motorcade, under a driver/vehicle/road integrated system.

As we know, traffic safety is the interaction results of human, vehicle, and environment. First, based on the essence of stability mechanism and nonlinear dynamic characteristics of tractor-semitrailer, advanced active control devices similar to ABS and ESC, should be developed and equipped, especially on slippery pavement. Second, large vehicle drivers' physiological and psychological characteristics should be paid more attention and it is necessary to research and apply ADAS (Advanced Driver Assistance Systems), such as fatigue warning, auxiliary brake, and Lane keeping assist system. Last but not least, with the development of Internet technology, ITS (Intelligent Traffic System) should be widely applied to build a harmonious running state.

Conflicts of Interest

The authors declare that there are no conflicts of interest regarding the publication of this article.

Acknowledgments

This work is partially supported by the National Natural Science Foundation of China (Grants nos. 51775565 and 51208500), the Tianjin Science and Technology Innovation Platform Plan (Grant no. 16PTGCCX00150), the National Natural Science Foundation of Tianjin (Key Program, Grant no. 16JCZDJC38200), the University Foundation of Tianjin University of Technology and Education (Grant no. KYQD 1710), the Opening Fund of Guangdong Key Laboratory of Intelligent Transportation System (Grant no. 201701002), and the project named as China New Energy Automobile Products Testing Conditions Research and Development with Guangzhou traffic condition data collection. The first author would like to thank Dr. Z. W. Guan and Dr. R. H. Zhang for valuable discussions to improve the quality and presentation of the paper.

References

[1] H. Troger and K. Zeman, "Application of bifurcation theory to tractor-semitrailer dynamics," *Vehicle System Dynamics*, vol. 10, no. 2-3, pp. 156–161, 1981.

[2] H. Troger and K. Zeman, "A nonlinear analysis of the generic types of loss of stability of the steady state motion of a tractor-semitrailer," *Vehicle System Dynamics*, vol. 13, no. 4, pp. 161–172, 1984.

[3] A. Dunn, *Jackknife stability of articulated tractor semitrailer vehicles with high-output brakes and jackknife detection on low coefficient surfaces [MSc. thesis]*, Ohio State University, Columbus, Ohio, USA, 2003.

[4] M.-W. Suh, Y.-K. Park, S.-J. Kwon, S.-H. Yang, and B.-C. Park, "A simulation program for the braking characteristics of tractor-semitrailer vehicle," *SAE Technical Papers*, vol. 9, no. 2, pp. 152–167, 2000.

[5] A. L. Dunn, C. B. Tanner, D. R. Morr et al., "The influence of disablement of various brakes on the dry stopping performance and stability of a tractor-semitrailer," *SAE International Journal of Commercial Vehicles*, vol. 2, no. 1, pp. 1–16, 2009.

[6] M. F. J. van de Molengraft-Luijten, I. J. M. Besselink, R. M. A. F. Verschuren, and H. Nijmeijer, "Analysis of the lateral dynamic behaviour of articulated commercial vehicles," *Vehicle System Dynamics*, vol. 50, supplement 1, pp. 169–189, 2012.

[7] X. Yang and J. Xiong, "Nonlinear yaw dynamics analysis and control for the tractor-semitrailer vehicle," *International Journal of Heavy Vehicle Systems*, vol. 20, no. 3, pp. 253–288, 2013.

[8] N. Ding, X. Shi, Y. Zhang, and W. Chen, "Analysis of bifurcation and stability for a tractor semi-trailer in planar motion," *Vehicle System Dynamics*, vol. 52, no. 12, pp. 1729–1751, 2014.

[9] S. Sadri and C. Wu, "Stability analysis of a nonlinear vehicle model in plane motion using the concept of Lyapunov exponents," *Vehicle System Dynamics*, vol. 51, no. 6, pp. 906–924, 2013.

[10] O. Polach and I. Kaiser, "Comparison of methods analyzing bifurcation and hunting of complex rail vehicle models," *Journal of Computational and Nonlinear Dynamics*, vol. 7, no. 4, Article ID 041005, 2012.

[11] X. W. Wu and M. R. Chi, "Parameters study of hopf bifurcation in railway vehicle system," *Journal of Computational Nonlinear Dynamics*, vol. 10, no. 3, pp. 43–53, 2014.

[12] S. Tousi, A. K. Bajaj, and W. Soedel, "Closed-loop directional stability of car-trailer combinations in straight-line motion," *Vehicle System Dynamics*, vol. 51, no. 6, pp. 906–924, 2013.

[13] Z. Liu, "Characterisation of optimal human driver model and stability of a tractor-semitrailer vehicle system with time delay," *Mechanical Systems and Signal Processing*, vol. 21, no. 5, pp. 2080–2098, 2007.

[14] M. Sarvi, "Heavy commercial vehicles-following behavior and interactions with different vehicle classes," *Journal of Advanced Transportation*, vol. 47, no. 6, pp. 572–580, 2013.

[15] G. Yu, P. Wang, X. Wu, and Y. Wang, "Linear and nonlinear stability analysis of a car-following model considering velocity difference of two adjacent lanes," *Nonlinear Dynamics*, vol. 84, no. 1, pp. 387–397, 2016.

[16] F. D. Rossa, M. Gobbi, G. Mastinu, C. Piccardi, and G. Previati, "Bifurcation analysis of a car and driver model," *Vehicle System Dynamics*, vol. 52, supplement 1, pp. 142–156, 2014.

[17] Z. Liu and G. Payre, "Global bifurcation analysis of a nonlinear road vehicle system," *Journal of Computational and Nonlinear Dynamics*, vol. 2, no. 4, pp. 308–315, 2007.

[18] S. Li, S. Yang, and L. Chen, "A nonlinear vehicle-road coupled model for dynamics research," *Journal of Computational and Nonlinear Dynamics*, vol. 8, no. 2, Article ID 21001, pp. 1–15, 2013.

[19] Z. Liu, K. Hu, and K.-W. Chung, "Nonlinear analysis of a closed-loop tractor-semitrailer vehicle system with time delay," *Mechanical Systems and Signal Processing*, vol. 76-77, pp. 696–711, 2016.

[20] I. Koglbauer, J. Holzinger, A. Eichberger, and C. Lex, "Drivers' interaction with adaptive cruise control on dry and snowy roads with various tire-road grip potentials," *Journal of Advanced Transportation*, vol. 2017, Article ID 5496837, 10 pages, 2017.

[21] Y. Bie, T. Z. Qiu, C. Zhang, and C. Zhang, "Introducing weather factor modelling into macro traffic state prediction," *Journal of Advanced Transportation*, vol. 2017, Article ID 4879170, 15 pages, 2017.

[22] T. Tang, C. Li, H. Huang, and H. Shang, "A new fundamental diagram theory with the individual difference of the driver's

perception ability," *Nonlinear Dynamics*, vol. 67, no. 3, pp. 2255–2265, 2012.

[23] T. Tang, Y. Wang, X. Yang, and Y. Wu, "A new car-following model accounting for varying road condition," *Nonlinear Dynamics*, vol. 70, no. 2, pp. 1397–1405, 2012.

[24] T.-Q. Tang, L. Caccetta, Y.-H. Wu, H.-J. Huang, and X.-B. Yang, "A macro model for traffic flow on road networks with varying road conditions," *Journal of Advanced Transportation*, vol. 48, no. 4, pp. 304–317, 2014.

[25] D. Ma, X. Luo, W. Li, S. Jin, W. Guo, and D. Wang, "Traffic demand estimation for lane groups at signal-controlled intersections using travel times from video-imaging detectors," *IET Intelligent Transport Systems*, vol. 11, no. 4, pp. 222–229, 2017.

[26] D. Ma, F. Fu, S. Jin et al., "Gating control for a single bottleneck link based on traffic load equilibrium," *International Journal of Civil Engineering*, vol. 14, no. 5, pp. 281–293, 2016.

[27] D. Ma, X. Luo, S. Jin, D. Wang, W. Guo, and F. Wang, "Lane-based saturation degree estimation for signalized intersections using travel time data," *IEEE Intelligent Transportation Systems Magazine*, vol. 9, no. 3, pp. 136–148, 2017.

[28] X. Lin, N. Ding, G. Xu, and F. Gao, "High speed optimal yaw stability of tractor-semitrailers with active trailer steering," *SAE Technical Papers*, vol. 1, 2014.

[29] L. Palkovics and M. El-Gindy, "Examination of different control strategies of heavy-vehicle performance," *Journal of Dynamic Systems, Measurement, and Control*, vol. 118, no. 3, pp. 489–497, 1996.

[30] S. Chang, H. G. Xu, and H. F. Liu, "H_∞ loop shaping robust controller design for tractor-semitrailer," *Journal of Jilin University*, vol. 41, no. 6, pp. 1571–1576, 2011.

[31] J. Liang, X. Yuan, Y. Yuan, Z. Chen, and Y. Li, "Nonlinear dynamic analysis and robust controller design for Francis hydraulic turbine regulating system with a straight-tube surge tank," *Mechanical Systems and Signal Processing*, vol. 85, pp. 927–946, 2017.

[32] H. Takenaga, M. Konishi, and J. Imai, "Route tracking control of tractor-trailer vehicles based on fuzzy controller," in *Proceedings of the 5th International Workshop on Computational Intelligence and Applications*, pp. 105–110, Higashihiroshima, Japan, November 2009.

[33] C. S. Chin, X. Ji, W. L. Woo, T. J. Kwee, and W. Yang, "Modified multiple generalized regression neural network models using fuzzy C-means with principal component analysis for noise prediction of offshore platform," *Neural Computing & Applications*, no. 6, pp. 1–16, 2017.

[34] X. Yang, J. Song, and J. Gao, "Fuzzy logic based control of the lateral stability of tractor semitrailer vehicle," *Mathematical Problems in Engineering*, vol. 2015, Article ID 692912, 16 pages, 2015.

[35] C. Zong, T. Zhu, C. Wang, and H. Liu, "Multi-objective stability control algorithm of heavy tractor semi-trailer based on differential braking," *Chinese Journal of Mechanical Engineering*, vol. 25, no. 1, pp. 88–97, 2012.

[36] Z.-Z. He, H. Qi, M.-J. He, and L.-M. Ruan, "Experimental research on the photobiological hydrogen production kinetics of Chlamydomonas reinhardtii GY-D55," *International Journal of Hydrogen Energy*, vol. 41, no. 35, pp. 15651–15660, 2016.

[37] R. Zhang, K. Li, Z. He, H. Wang, and F. You, "Advanced emergency braking control based on a nonlinear model predictive algorithm for intelligent vehicles," *Applied Sciences*, vol. 7, no. 5, pp. 504–522, 2017.

[38] H. Xiao, R. Cui, and D. Xu, "A sampling-based bayesian approach for cooperative multiagent online search with resource constraints," *IEEE Transactions on Cybernetics*, 2017.

[39] F. You, R. Zhang, G. Lie, H. Wang, H. Wen, and J. Xu, "Trajectory planning and tracking control for autonomous lane change maneuver based on the cooperative vehicle infrastructure system," *Expert Systems with Applications*, vol. 42, no. 14, pp. 5932–5946, 2015.

[40] Z. Liu, Y. Zhang, S. Wang, and Z. Li, "A trial-and-error method with autonomous vehicle-to-infrastructure traffic counts for cordon-based congestion pricing," *Journal of Advanced Transportation*, vol. 2017, Article ID 9243039, 8 pages, 2017.

[41] J. Wang, C. Wang, J. Lv, Z. Zhang, and C. Li, "Modeling travel time reliability of road network considering connected vehicle guidance characteristics indexes," *Journal of Advanced Transportation*, vol. 2017, Article ID 2415312, 9 pages, 2017.

[42] C. S. Chin, W. Atmodihardjo, L. W. Woo, and E. Mesbahi, "Remote temperature monitoring device using a multiple patients-coordinator set design approach," *ROBOMECH Journal*, vol. 2, no. 1, pp. 1–9, 2015.

[43] R. Zhang, J. Wu, L. Huang, and F. You, "Study of bicycle movements in conflicts at mixed traffic unsignalized intersections," *IEEE Access*, vol. 5, pp. 10108–10117, 2017.

[44] P. Chen, W. Zeng, G. Yu, and Y. Wang, "Surrogate safety analysis of pedestrian-vehicle conflict at intersections using unmanned aerial vehicle videos," *Journal of Advanced Transportation*, vol. 2017, Article ID 5202150, 12 pages, 2017.

[45] C. S. Chin, W. P. Lin, and J. Y. Lin, "Experimental validation of open-frame ROV model for virtual reality simulation and control," *Journal of Marine Science & Technology*, no. 2, pp. 1–21, 2017.

[46] F.-C. Wang and W.-H. Fang, "The development of a PEMFC hybrid power electric vehicle with automatic sodium borohydride hydrogen generation," *International Journal of Hydrogen Energy*, vol. 42, no. 15, pp. 10376–10389, 2017.

[47] W. Lin and C. S. Chin, "Block diagonal dominant remotely operated vehicle model simulation using decentralized model predictive control," *Advances in Mechanical Engineering*, vol. 9, no. 4, pp. 1–24, 2017.

[48] D. K. Kim, H. E. Min, I. M. Kong et al., "Parametric study on interaction of blower and back pressure control valve for a 80-kW class PEM fuel cell vehicle," *International Journal of Hydrogen Energy*, vol. 41, no. 39, pp. 17595–17615, 2016.

[49] F. Tazerart, Z. Mokrani, D. Rekioua, and T. Rekioua, "Direct torque control implementation with losses minimization of induction motor for electric vehicle applications with high operating life of the battery," *International Journal of Hydrogen Energy*, vol. 40, no. 39, pp. 13827–13838, 2015.

[50] R. Zhang, Z. He, H. Wang, F. You, and K. Li, "Study on self-tuning tyre friction control for developing main-servo loop integrated chassis control system," *IEEE Access*, vol. 5, pp. 6649–6660, 2017.

[51] P. Huynh, T.-H. Do, and M. Yoo, "A probability-based algorithm using image sensors to track the LED in a vehicle visible light communication system," *Sensors*, vol. 17, no. 2, pp. 347–357, 2017.

[52] R. Huang, H. Liang, P. Zhao, B. Yu, and X. Geng, "Intent-estimation- and motion-model-based collision avoidance method for autonomous vehicles in urban environments," *Applied Sciences*, vol. 7, no. 5, p. 457, 2017.

[53] B. Gao, R. Zhang, and X. Lou, "Modeling day-to-day flow dynamics on degradable transport network," *PLoS ONE*, vol. 11, no. 12, Article ID e0168241, 2016.

[54] V. V. Dixit, S. Chand, and D. J. Nair, "Autonomous vehicles: disengagements, accidents and reaction times," *PLoS ONE*, vol. 11, no. 12, Article ID 0168054, 2016.

[55] D. Ahn, H. Park, S. Hwang, and T. Park, "Reliable identification of vehicle-boarding actions based on fuzzy inference system," *Sensors*, vol. 17, no. 2, pp. 333–342, 2017.

[56] R. Dai, Y. Lu, C. Ding, and G. Lu, "The effect of connected vehicle environment on global travel efficiency and its optimal penetration rate," *Journal of Advanced Transportation*, vol. 2017, Article ID 2697678, 10 pages, 2017.

[57] W. Sun, X. Wu, Y. Wang, and G. Yu, "A continuous-flow-intersection-lite design and traffic control for oversaturated bottleneck intersections," *Transportation Research Part C: Emerging Technologies*, vol. 56, pp. 18–33, 2015.

[58] X. Wu, X. He, G. Yu, A. Harmandayan, and Y. Wang, "Energy-optimal speed control for electric vehicles on signalized arterials," *IEEE Transactions on Intelligent Transportation Systems*, vol. 16, no. 5, pp. 2786–2796, 2015.

[59] H. Li, C. Li, H. Li, Y. Li, and Z. Xing, "An integrated altitude control design for a tail-sitter UAV equipped with turbine engines," *IEEE Access*, vol. 5, pp. 10941–10952, 2017.

[60] X. Bao, H. Li, D. Xu, L. Jia, B. Ran, and J. Rong, "Traffic vehicle counting in jam flow conditions using low-cost and energy-efficient wireless magnetic sensors," *Sensors*, vol. 16, no. 11, pp. 1868–1883, 2016.

[61] M. Ibarra-Arenado, T. Tjahjadi, J. Pérez-Oria, S. Robla-Gómez, and A. Jiménez-Avello, "Shadow-based vehicle detection in Urban traffic," *Sensors*, vol. 17, no. 5, pp. 975–993, 2017.

[62] M. Da Lio, F. Biral, E. Bertolazzi et al., "Artificial co-drivers as a universal enabling technology for future intelligent vehicles and transportation systems," *IEEE Transactions on Intelligent Transportation Systems*, vol. 16, no. 1, pp. 244–263, 2015.

[63] T. Yin, D. Huang, and S. Fu, "Adaptive decision and robust control under parallel precedence constraints in human strategy modeling," *IEEE Access*, vol. 5, pp. 9944–9956, 2017.

[64] Z. S. Yu, Z. F. Wang, and W. Y. Wang, *Handbook of Mechanical Engineering*, China Communications Press, Beijing, China, 2003.

[65] H. B. Pacejka, *Tire and Vehicle Dynamics*, Butterworth-Heinemann, London, UK, 2012.

[66] E. Bakker, L. Nyborg, and H. B. Pacejka, "Tyre modelling for use in vehicle dynamics studies," *SAE Technical Papers*, Article ID 870421, pp. 1–15, 1987.

[67] H. Toger and A. Steindl, *Nonlinear Dynamic Introduction*, Springer-Verlag Press, Berlin, Germany, 2012.

[68] Q. C. Zhang, H. L. Wang, and Z. W. Zhu, *Bifurcation and Chaos Theory and Application*, Tianjin University Press, Tianjin, China, 2005.

[69] D. P. Li, *Nonlinear Control System*, Northwestern Polytechnical University Press, Xi'an, China, 2009.

[70] S. Tippaya, S. Sitjongsataporn, T. Tan, M. M. Khan, and K. Chamnongthai, "Multi-modal visual features-based video shot boundary detection," *IEEE Access*, vol. 5, pp. 12563–12575, 2017.

[71] O. Ur-Rehman and N. Zivic, "Two-phase method for image authentication and enhanced decoding," *IEEE Access*, vol. 5, pp. 12158–12167, 2017.

[72] R. Zhang, Y. Ma, F. You, T. Peng, Z. He, and K. Li, "Exploring to direct the reaction pathway for hydrogenation of levulinic acid into γ-valerolactone for future Clean-Energy Vehicles over a magnetic Cu-Ni catalyst," *International Journal of Hydrogen Energy*, vol. 42, no. 40, pp. 25185–25194, 2017.